

Short Communication

Hydrogen Embrittlement Behavior of Ultrahigh Strength Mooring Chain Steel Evaluated by the Slow Strain Rate Test

Songjie Li¹, Jiang Yin², Chengduo Wang^{3,*}, Cuihong Hou¹, Fan Li¹

¹ School of Chemical Engineering and Energy, Zhengzhou University, 100 Science Avenue, Zhengzhou, Henan 450001, China;

² Asian Star Anchor Chain Co., Ltd., Jingjiang, Jiangsu 214533, China;

³ School of Material Science and Engineering, Zhengzhou University, 100 Science Avenue, Zhengzhou, Henan 450001, China

*E-mail: wangchengduo@163.com

Received: 9 November 2018 / Accepted: 20 December 2018 / Published: 7 February 2019

In this study, the hydrogen embrittlement behavior of an ultrahigh strength mooring chain steel with a tensile strength of 1150 MPa was evaluated. The hydrogen was precharged into the notched specimen by electrochemical hydrogen charging. The fracture stress and hydrogen content were obtained by a slow strain rate test (SSRT) and thermal desorption analysis (TDA). The results show that the fracture stress decreased linearly with hydrogen content when the hydrogen content was less than 2.0 wppm. At this point, the intergranular fracture occurred, where the fracture stress as a function of hydrogen content changed from a linear to a power law relationship. The maximum hydrogen content from the corrosive environment was 1.4 wppm, which is lower than that of the onset of intergranular fracture at a diffusible hydrogen content of 2.0 wppm. The precharged hydrogen was possibly trapped by the grain boundaries.

Keywords: hydrogen embrittlement; mooring chain steel; thermal desorption analysis; slow strain rate test

1. INTRODUCTION

Recently, increasing attention has been placed on energy sources at deep water locations because of the increasing demand for oil and gas. When exploring in the deep ocean, a longer mooring chain is required to ensure the safety of the platform. The added weight of a longer chain requires a higher strength for the mooring chain steel. However, it is well known that high strength steel is susceptible to hydrogen in terms of hydrogen embrittlement (HE) [1-9]. Many studies on the hydrogen embrittlement of high strength steels have been conducted in the past several decades [10-19]. It is known that diffusible

hydrogen in steels plays an important role in the hydrogen embrittlement of high strength steel [20-22]. In addition, the degradation of mechanical properties because of HE increases with increasing strength.

There are two main ways for hydrogen to enter the mooring chain. One is from hydrogen formed by the cathodic reactions in marine corrosion, and the other is the inappropriate operation of cathodic protection systems that results from the application of excessive negative potentials [23-28]. Mooring chain steels with tensile strengths over 690 MPa are generally regarded as high strength. Although high strength steels are increasingly used in deep sea environment, basic research on the hydrogen embrittlement of high strength mooring chain steels is still relatively scarce but urgently needed to supplement for the safe engineering design of mooring systems.

In a previous study, the critical diffusible hydrogen content leading to fracture for high strength steels was obtained by precharging electrochemical hydrogen into specimens and using a slow strain rate test (SSRT) [29-31], a constant load test (CLT) [32-33], and a conventional strain rate test (CSRT) [34-35]. In this study, to clarify the influence of hydrogen on the hydrogen embrittlement behavior of ultrahigh strength mooring chain steel, the SSRT combined thermal desorption analysis (TDA) was conducted for electrochemical hydrogen precharged notched bar specimens. For comparison with the critical hydrogen content for fracture, the environmental hydrogen entry for the round bar specimens corroded in a pH 2 HCl solution was also measured by TDA.

2. EXPERIMENTAL PROCEDURES

A newly developed ultrahigh strength mooring chain steel with the nominal composition of 0.22C-0.25Si-0.30Mn-4.9(Cr+Ni+Mo)-0.15(V+Nb+Ti) and a tensile strength of 1200 MPa was used in this study. The circumferentially notched round bar specimens were used for SSRTs with the dimensions shown in Fig. 1. The calculated stress concentration factor, K_t , was 4.9 [36].

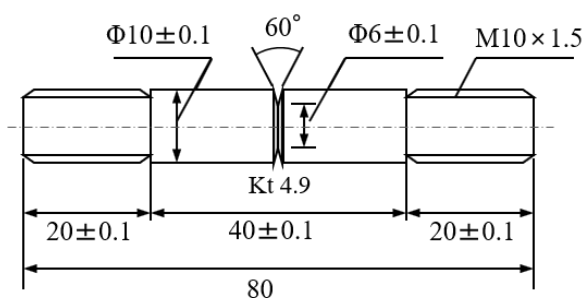


Figure 1. Dimensions (in mm) of a circumferentially notched round bar specimen with the notch root radius of 0.1 mm for a K_t of 4.9.

To clarify the change in the hydrogen charging time with hydrogen content for SSRT specimens, a round bar specimen with a length of 20 mm and diameter of 10 mm was used for the hydrogen precharging in 0.1 mol/L NaOH solution with a current density of 10 A/m² from 24 h to 96 h, and then the hydrogen content was measured by TDA.

A round bar specimen with a length of 40 mm and a diameter of 7 mm was used to investigate

the hydrogen entry from corrosive environment. The specimen was immersed in a HCl solution with a pH of 2 at 30 °C, and the solution was changed every three days. Then the hydrogen content was measured by TDA.

For the SSRT, the hydrogen was introduced into the specimens by electrochemically precharging in a 0.1 mol/L NaOH aqueous solution, with a the current density of 1-20 A/m². The SSRT for the charged specimen was conducted on a WDML-300 kN slow tensile testing machine, with a constant crosshead speed of 0.005 mm/min corresponding to a nominal strain rate of 8.3×10⁻⁷ s⁻¹. The fracture stress was calculated as $\sigma_f = F_{\max}/A_{\min}$, where F_{\max} is the maximum tensile strength and A_{\min} is the cross-section area around the notch. The specimens fractured after the SSRT for approximately 6 h and were immediately kept in liquid nitrogen until the hydrogen was measured by TDA.

The hydrogen content in the specimen after fracture from the SSRT was measured by TDA using an instrument developed by R-Dec Co. Ltd. The TDA was conducted from ambient temperature to 1073K to obtain hydrogen desorption spectra with heating rate of 100 K h⁻¹. As reported by Takai and Watanuki, the hydrogen diffusing in the specimen (H_D) is regarded as playing an important role in hydrogen embrittlement. The typical hydrogen desorption curve obtained by TDA for the mooring chain steel is shown in Fig. 2. The peak appearing up to 460K was regarded as diffusible hydrogen and the hydrogen content was calculated from room temperature to 600K of the spectrum.

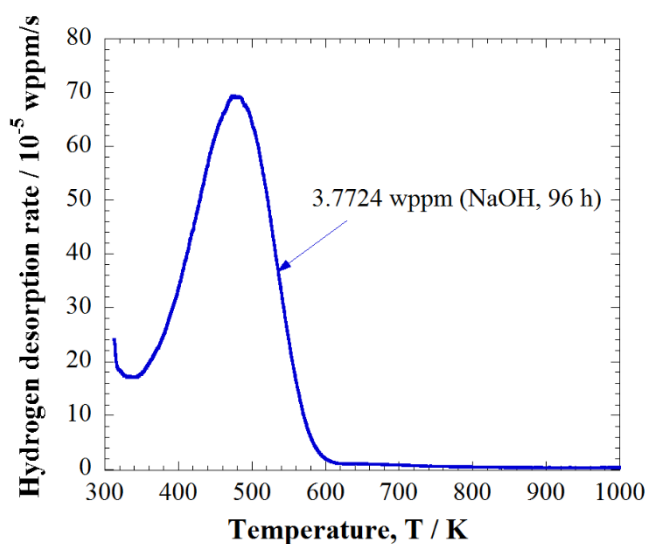


Figure 2. A typical hydrogen desorption curve for mooring chain steel for the specimen electrochemical hydrogen precharging in a 0.1 mol/L NaOH solution for 96 h with hydrogen charge current density of 10 A/m².

The polished specimens were etched with a 2% nital solution, and their microstructure was observed on a METAVAL optical microscope. After the specimen fractured, the fracture surface was observed on a JSM 7500F scanning electron microscope (SEM), operating at 15 kV.

3. RESULTS AND DISCUSSION

The optical micrographs of the ultrahigh strength mooring chain steel are shown in Fig. 3. We

can see that the ferrite grain is only approximately $10\ \mu\text{m}$, and the finer carbide precipitates (black dots) are uniformly dispersed in the matrix, which indicates a microstructure of tempered sorbite.

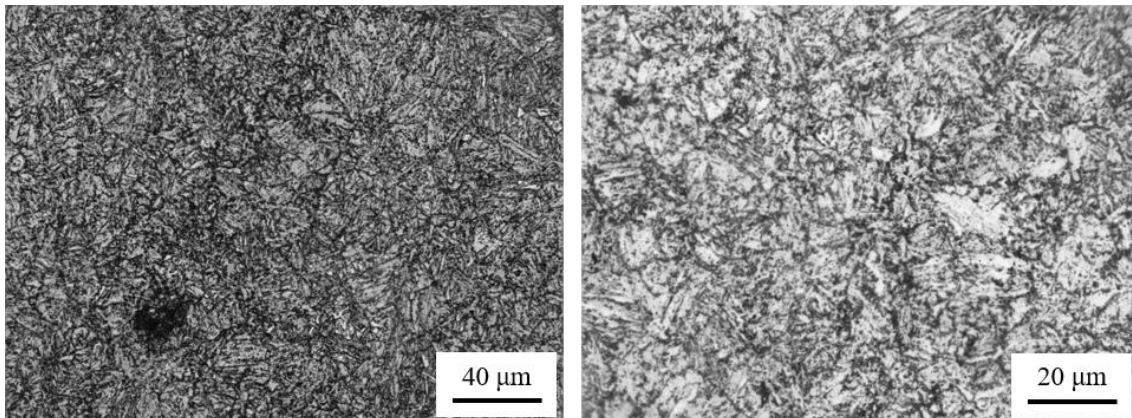


Figure 3. Optical microscopy images for high strength mooring chain steel.

Fig. 4 shows the change in the hydrogen content with the hydrogen charging time in a $0.1\ \text{mol/L}$ NaOH solution at a current density of $10\ \text{A/m}^2$. The hydrogen content increased with increasing charge time. The hydrogen content remained almost constant after 72 h and did not change much for the 72 h and 96 h charged specimens. Thus, to obtain homogeneous hydrogen in the sample, all the SSRT specimens in the study were charged for 96 h in $0.1\ \text{mol/L}$ NaOH solution.

Fig. 5 shows the TDA curves for the specimens after the SSRT. There is hydrogen desorption peak for the specimen without hydrogen charging, while a clear hydrogen desorption peak appears at approximately 460K for the hydrogen charged specimen. The hydrogen content increased as the charging current density increased.

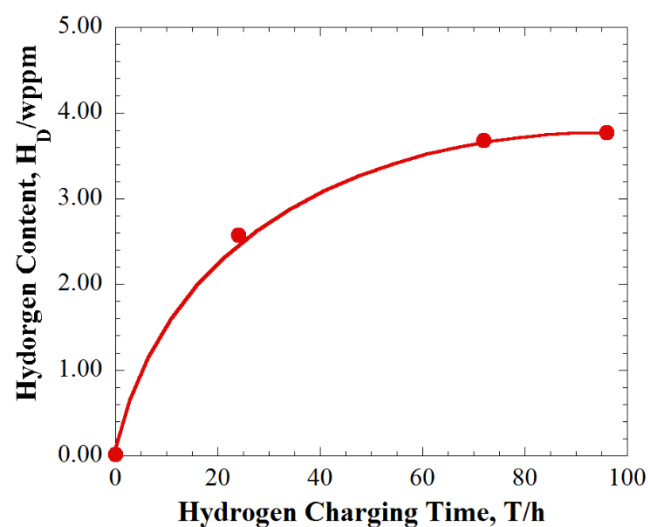


Figure 4. Effect of hydrogen charging time on hydrogen content in a $0.1\ \text{mol/L}$ NaOH aqueous solution at a current density of $10\ \text{A/m}^2$

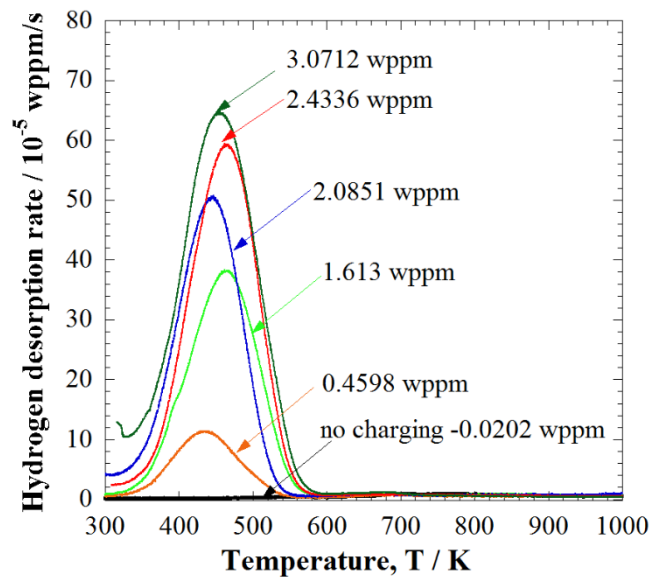


Figure 5. TDA curves of notched specimens with hydrogen precharged in a 0.1 mol/L NaOH aqueous solution measured after the SSRT.

Fig.6. shows the dependence of fracture stress on diffusible hydrogen content for hydrogen precharged ultrahigh strength mooring chain steel specimens. For comparison, the corresponding data for AISI 4135 steels with a tensile strength of 1300 MPa (B13) are also plotted [29]. The fracture stress of ultrahigh strength mooring chain steel decreased with increasing hydrogen content. As the precharged hydrogen content was less than 2.0 wppm, the maximum fracture stress decreased linearly with increasing hydrogen content. When the diffusible hydrogen content increases to above 2.0 wppm, the maximum tensile stress decreased drastically such as that of the B13 specimen, which is similar to most other high-strength steel with hydrogen embrittlement obtained from the evaluation based on the hydrogen content [5,30-31,37]. This is probably due to the structure resistance to hydrogen embrittlement.

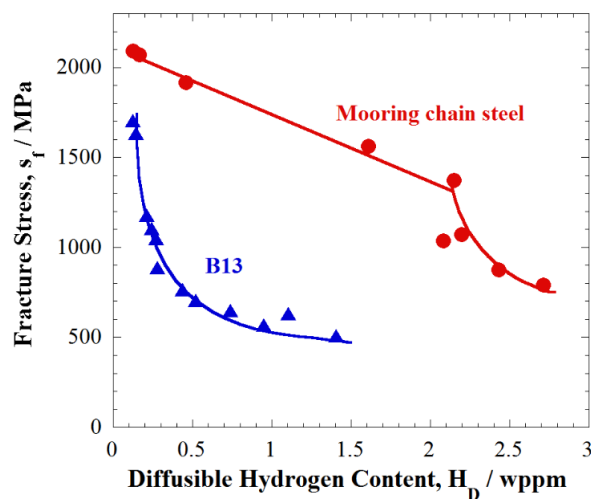


Figure 6. Dependence of fracture stress on diffusible hydrogen content after the SSRT for mooring chain steel specimens

The typical fracture surfaces of specimens observed by SEM after the SSRT are shown in Fig. 7. For the specimen without charging (Fig. 7a), no diffusible hydrogen content was detected, indicating a ductile fracture mode. The embrittlement dependence on the hydrogen content was caused by the amount of diffusible hydrogen in the specimen as shown in Fig. 7b-7f. Quasi-cleavage (QC) was found in the specimens with a charged hydrogen content of 1.6 wppm (Fig. 7c). Intergranular fracture (IG) occurred when the hydrogen content reached 2.0 wppm (Fig. 7d). The ratio of intergranular fracture was increased with increasing hydrogen content as shown in Fig. 7f. For the high strength mooring chain steel in this study, the hydrogen content for the occurrence of QC and IG was much higher than that of a previous study with similar evaluation methods [11,31,38].

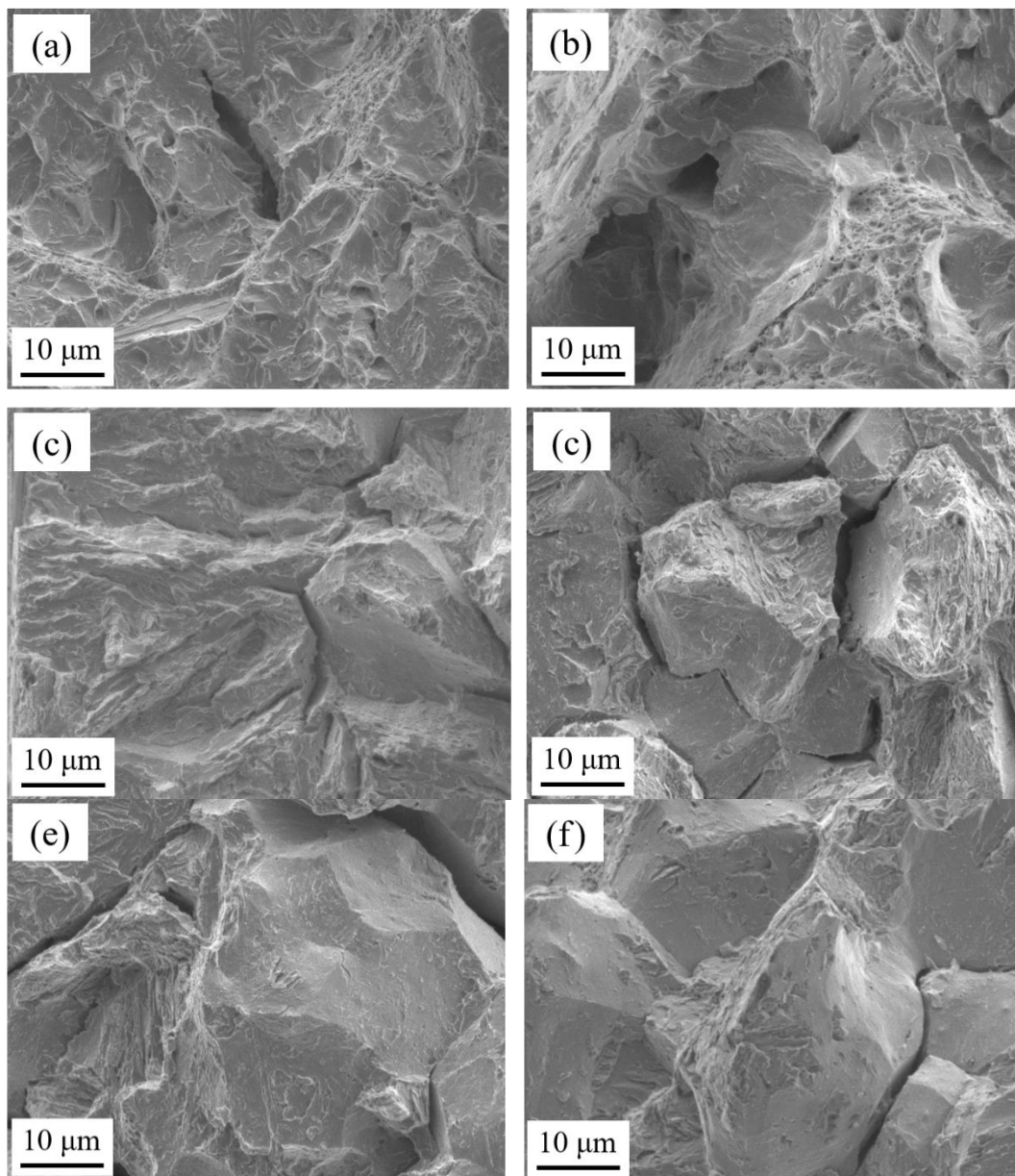


Figure 7. SEM images of mooring chain steel specimens with different hydrogen contents: (a) H_D -0.02, (b) H_D -0.46 wppm, (c) H_D -1.6 wppm, (d) H_D -2.0 wppm, (e) H_D -2.7 wppm, and (f) H_D -3.1 wppm.

For the mooring chain steel in this study, the critical hydrogen content was 2.0 wppm for the occurrence of IG, which is the turning point for the fracture stress from a linear to a power law relationship, as shown in Fig. 6. Thus, the onset of IG fracture at a hydrogen content over 2.0 wppm is in agreement with the rapid decrease in the fracture stress, as shown in Fig. 7e and 7f. As revealed by TDS, the strength of the grain boundary decreased more rapidly than that of the interior grain strength. With a certain hydrogen content the interior grain strength may be less than the strength of the grain boundaries, which determine the fracture stress. Thus, it can be assumed that the diffusible hydrogen was trapped in grain boundaries [30].

It has been proven that hydrogen entry from corrosive environments plays an important role in the hydrogen embrittlement of high strength steel [13]. To compare the critical hydrogen content from hydrogen charging with hydrogen content from a severe corrosive environment, the mooring chain steel specimen was immersed in a pH 2 HCl solution, and the hydrogen content was measured by TDA after different immersing times. The change of hydrogen content with corrosive time in pH 2 HCl solution is shown in Fig. 8. The hydrogen content increased with immersion time, and after 30 days, it achieved a constant value of 1.4 wppm. Based on a previous study [37,39-41], for AISI 4135 and hydrogen trapping steel, the hydrogen content entering from atmospheric and marine environmental corrosion is much lower than that of the cyclic corrosion test for which the environment is more corrosive. The corrosion should be much more severe in a pH 2 HCl solution compared with the general corrosion environment, and the hydrogen entry is much easier in this study. In atmospheric or marine environments, the hydrogen content is assumed to be less than 1.4 wppm, which is lower than the turning point of 2 wppm from the precharged hydrogen content. To some extent, ultrahigh strength mooring chain steel should be less susceptible to hydrogen embrittlement based on the present study.

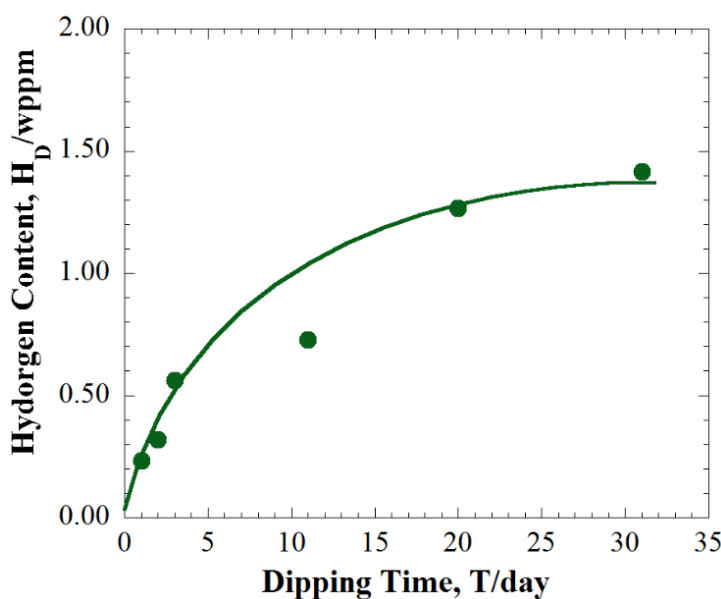


Figure 8. Change of hydrogen content with immersion time for the mooring chain steel specimen in a pH 2 HCl solution

4. SUMMARY

The hydrogen embrittlement of an ultrahigh strength mooring chain steel with the tensile strength of 1200 MPa was investigated. The slow strain rate test combined with hydrogen content obtained by thermal desorption analysis was used for hydrogen precharged specimens with a diffusible hydrogen content up to 3.1 wppm. The results show that the ultrahigh strength mooring chain steel used in the study had a high critical diffusible hydrogen content for hydrogen embrittlement. The hydrogen in the steel was trapped by grain boundaries. The fracture stress decreases linearly when the hydrogen content was less than 2.0 wppm, and it showed a power law relationship concomitant with brittle intergranular fracture with increasing hydrogen content. The maximum hydrogen content from a severe corrosive environment is 1.4 wppm, which is lower than that of the intergranular fracture mode that occurred at a hydrogen content of 2.0 wppm.

ACKNOWLEDGMENTS

This work is partially supported by a grant from the National Natural Science Foundation of China (Grant no. 51601170) and Key Scientific Research Project of Colleges and Universities in Henan Province (No. 17A430029). These grants are gratefully acknowledged.

References

1. J.P. Hirth, *Metall. Trans. A*, 11 (1980) 861.
2. M. Nagumo, *Mater. Sci. Tech-lond.*, 20 (2004) 940.
3. X. Li, J. Zhang, Q. Fu, X. Song, S. Shen and Q. Li, *Mater. Sci. Eng. A*, 724 (2018) 518.
4. T. Tsuru, Y. Huang, M.R. Ali and A. Nishikata, *Corros. Sci.*, 47 (2005) 2431.
5. M.Q. Wang, E. Akiyama and K. Tsuzaki, *Corros. Sci.*, 49 (2007) 4081.
6. Y.-S. Chen, D. Haley, S.S.A. Gerstl, A.J. London, F. Sweeney, R.A. Wepf, W.M. Rainforth, P.A.J. Bagot and M.P. Moody, *Science*, 355 (2017) 1196.
7. H. Bhadeshia, *ISIJ Int.*, 56 (2016) 24.
8. M. Koyama, E. Akiyama, Y.-K. Lee, D. Raabe and K. Tsuzaki, *Int. J. Hydrogen Energy*, 42 (2017) 12706.
9. Y. Matsumoto and K. Takai, *Metall. Mater. Trans. A*, 490 (2018) 490.
10. M. Moshref-Javadi, H. Edris, A. Shafyei and H. Salimi-Jazi, *Int. J. hydrogen energy*, 42 (2017) 6409.
11. J.S. Kim, Y.H. Lee, D.L. Lee, K.-T. Park and C.S. Lee, *Mater. Sci. Eng. A*, 505 (2009) 105.
12. F.G. Wei and K. Tsuzaki, *Metall. Mater. Trans. A*, 37 (2006) 331.
13. S.J. Li, Z.G. Zhang and E. Akiyama, K. Tsuzaki, B. Zhang. *Corros. Sci.*, 52 (2010) 1660.
14. E. Akiyama, S.J. Li and T. Shinohara, Z. Zhanga, K. Tsuzakia. *Electrochim. Acta*, 56 (2011) 1799.
15. D.H. Shim, T. Lee, J. Lee, H.J. Lee, J.-Y. Yoo and C.S. Lee, *Mater. Sci. Eng. A*, 700 (2017) 473.
16. K. Takashima, Y. Yoshikoka, K. Yokoyama and Y. Funakawa, *ISIJ Int.*, 58 (2018) 173.
17. L. Cho, E.J. Seo, D.H. Sulistiyo, K.R. Jo, S.W. Kim, J.K. Oh, Y.R. Cho and B.C.D. Cooman, *Mater. Sci. Eng. A*, 735 (2018) 448.
18. Q. Liu, Q. Zhou and J. Venezuela. *Mater. Sci. Eng. A*, 715 (2018) 370.
19. X. Li, J. Zhang, E. Akiyama, Y. Wang and Q. Li, *Int. J. hydrogen energy*, 43 (2018) 17898.
20. K. Takai and R. Watanuki, *ISIJ Int.*, 43 (2003) 520.
21. N. Suzuki, N. Ishii, T. Miyagawa and H. Harada, *Tetsu-to-Hagané*, 79 (1993) 227.
22. S. Yamasaki and T. Takahashi, *Tetsu-to-Hagané*, 83 (1997) 454.
23. M. Robinson and P. Kilgallon, *Corros. Sci.*, 50 (1994) 626.

24. J. Ćwiek and K. Nikiforov, *Mater. Sci.*, 40 (2004) 831.
25. M.S. Han, J.C. Park, S.K. Jang and S.J. Kim, *Phys. Scripta*, T139 (2010) 014037.
26. H. Ma, Z. Liu, C. Du, H. Wang, C. Li and X. Li, *Mater. Sci. Eng. A*, 642 (2015) 22.
27. R. Francis, G. Byrne and G.R. Warburton, *Corrosion*, 53 (1997) 234.
28. T. Zhang, W. Zhao, T. Li, Y. Zhao, Q. Deng, Y. Wang and W. Jiang, *Corros. Sci.*, 131 (2018) 104.
29. M. Wang, E. Akiyama and K. Tsuzaki, *Mater. Sci. Eng. A*, 398 (2005) 37.
30. M. Wang, E. Akiyama and K. Tsuzaki, *Scripta Mater.*, 52 (2005) 403.
31. M. Wang, E. Akiyama and K. Tsuzaki, *Scripta Mater.*, 53 (2005) 713.
32. K. Hirai, K. Wakiyama and N. Uno, *J. Struct. Constr. Eng. AIJ*, 490 (1996) 215.
33. K. Hirai and N. Uno, *J. Struct. Constr. Eng. AIJ*, 560 (2002) 197.
34. Y. Hagihara, C. Ito, N. Hisamori, H. Suziki, K. Takai and E. Akiyama, *Tetsu-to-Hagané*, 94 (2008) 215.
35. Y. Hagihara, C. Ito, D. Kirikae, N. Hisamori, H. Suziki and K. Takai, *Tetsu-to-Hagané*, 95 (2009) 489.
36. S. Takagi, S. Terasaki, K. Tsuzaki, T. Inoue and F. Minami, *ISIJ Int.*, 45 (2005) 263.
37. S. Li, E. Akiyama, K. Yuuji, K. Tsuzaki, N. Uno and B. Zhang, *Sci. Technol. Adv. Mater.*, 11 (2010) 025005.
38. W. Hui, Z. Xu, Y. Zhang, X. Zhao, C. Shao, Y. Weng, *Mater. Sci. Eng. A*, 704 (2017) 199.
39. T. Omura, T. Kushida, F. Nakasato, S. Watanabe, I. Oyamada, *Tetsu-to-Hagane*, 91 (2005) 478.
40. T. Kushida, *ISIJ Int.*, 43(2003) 470.
41. E. Akiyama, K. Matsukado, M. Wang, K. Tsuzaki, *Corro. Sci.*, 52 (2010) 2758.